Free Radical Biology and Medicine 120 (2018) 1–12

Contents lists available at ScienceDirect

Free Radical Biology and Medicine

journal homepage: www.elsevier.com/locate/freeradbiomed

Original article

Downregulation of glycine decarboxylase enhanced cofilin-mediated migration in hepatocellular carcinoma cells

Hao Zhuang[a,b,c,1], Qiang Li[c,1], Xinran Zhang[a], Xuda Ma[a], Zun Wang[a], Yun Liu[a], Xianfu Yi[d], Ruibing Chen[a], Feng Han[b], Ning Zhang[a,*], Yongmei Li[a,*]

[a] Key Laboratory of Breast Cancer Prevention and Therapy, Laboratory of Cancer Cell Biology, Tianjin Medical University Cancer Institute and Hospital, Department of Pathogen Biology & Department of Genetics, School of Basic Medical Sciences, Tianjin Medical University, Tianjin 300070, China
[b] Department of Hepatic Biliary Pancreatic Surgery, Cancer Hospital Affiliated to Zhengzhou University, Zhengzhou, Henan Province 450000, China
[c] Department of Hepatobiliary Surgery, Tianjin Medical University Cancer Institute and Hospital, Tianjin 300070, China
[d] School of Biomedical Engineering, Tianjin Medical University, Tianjin 300070, China

ARTICLE INFO

Keywords:
Metastasis
ROS
Glycine
Glutathione
Cofilin

ABSTRACT

Metabolic reprogramming is a hallmark of cancer. Glycine decarboxylase (GLDC), an oxidoreductase, plays an important role in amino acid metabolism. While GLDC promotes tumor initiation and proliferation in non-small cell lung cancer and glioma and it was reported as a putative tumor suppressor gene in gastric cancer, the role of GLDC in hepatocellular carcinoma (HCC) is unknown. In the current study, microarray-based analysis suggested that GLDC expression was low in highly malignant HCC cell lines, and clinicopathological analysis revealed a decrease in GLDC in HCC tumor samples. While the knockdown of GLDC enhanced cancer cell migration and invasion, GLDC overexpression inhibited them. Mechanistic studies revealed that GLDC knockdown increased the levels of reactive oxygen species (ROS) and decreased the ratio of glutathione/oxidized glutathione (GSH/GSSG), which in turn dampened the ubiquitination of cofilin, a key regulator of actin polymerization. Consequently, the protein level of cofilin was elevated, which accounted for the increase in cell migration. The overexpression of GLDC reversed the phenotype. Treatment with N-acetyl-L-cysteine decreased the protein level of cofilin while treatment with H_2O_2 increased it, further confirming the role of ROS in regulating cofilin degradation. In a tumor xenographic transplant nude mouse model, the knockdown of GLDC promoted intrahepatic metastasis of HCC while GLDC overexpression inhibited it. Our data indicate that GLDC downregulation decreases ROS-mediated ubiquitination of cofilin to enhance HCC progression and intrahepatic metastasis.

1. Introduction

Liver cancer is the sixth most frequently diagnosed type of cancer and it has become the second-leading cause of cancer deaths worldwide [1]. Hepatocellular carcinoma (HCC) accounts for over 75% of liver malignancies [2,3]. Surgical resection is considered as the first choice and a curative treatment modality for HCC. However, a high incidence of postoperative tumor recurrence results in poor survival, and this is responsible for more than 90% of HCC deaths [4,5]. Intrahepatic metastasis is the major cause of postoperative recurrence [6]; therefore, it is critical to elucidate the metastatic factors and to understand the underlying molecular mechanism that is involved in HCC metastasis.

Metabolic reprogramming is a hallmark of cancer [7]. It has been well documented that cancer cells adopt altered carbohydrate and nucleotide metabolism for proliferation and metastasis [8,9]. Recently, several reports began to unveil the importance of amino acid metabolism during tumorigenesis [10–14]. It has been documented that glycine plays a pivotal role in rapid cancer cell proliferation [11] and

Abbreviations: 5,10-CH_2-THF, 5,10-methylene-tetrahydrofolate; CHX, cycloheximide; C, HCC tissues; DAPI, 4,6′-diamidino-2-phenylindole; DCFH-DA, 2′,7′-Dichlorofluorescin diacetate; DMEM, Dulbecco's modified Eagle medium; ECL, enhanced chemiluminescence; EGF, epidermal growth factor; FBS, fetal bovine serum; GLDC, glycine decarboxylase; HBsAg, hepatitis B surface antigen; HCC, hepatocellular carcinoma; HEPES, N-2-hydroxyethylpiperazine-N-2-ethane sulfonic acid; HR, hazard ratio; KEGG, Kyoto Encyclopedia of Genes and Genomes; LIMK, LIM kinase; MFI, mean fluorescence intensities; NAC, N-acetyl-L-cysteine; NSCLC, non-small cell lung cancer; OS, overall survival; P, para-tumor tissues; qRT-PCR, quantitative reverse transcription PCR; ROS, reactive oxygen species; SSH1, slingshot protein phosphatase 1; TCGA, The Cancer Genome Atlas

* Corresponding authors at: Key Laboratory of Breast Cancer Prevention and Therapy, Laboratory of Cancer Cell Biology, Tianjin Medical University Cancer Institute and Hospital, Department of Pathogen Biology & Department of Genetics, School of Basic Medical Sciences, Tianjin Medical University, Tianjin 300070, China.
E-mail addresses: zhangning@tmu.edu.cn (N. Zhang), liym@tmu.edu.cn (Y. Li).
[1] These authors contributed equally to this work.

https://doi.org/10.1016/j.freeradbiomed.2018.03.003
Received 30 June 2017; Received in revised form 1 March 2018; Accepted 3 March 2018
Available online 07 March 2018
0891-5849/

serine hydroxymethyltransferase 2 drives glioma cell survival [13]; however, the roles of amino acids and their metabolism in tumorigenesis and metastasis are still largely unknown.

Glycine decarboxylase (GLDC) is an oxidoreductase that catalyzes the irreversible rate-limiting step of glycine catabolism. Defects in GLDC cause nonketotic hyperglycinemia, an autosomal recessive inborn error [15]. Intracellular glycine is catalyzed by GLDC to generate carbon dioxide, ammonia, and 5,10-methylene-tetrahydrofolate (5,10-CH_2-THF), which drives *de novo* nucleotide biosynthesis and cellular methylation reactions during cell proliferation [16,17]. Meanwhile, glycine is also catalyzed by glutathione (GSH) synthetase to be incorporated into GSH [18]. GSH is an important modulator of cellular functions, including antioxidant defense via the direct interaction with reactive oxygen species (ROS) [19].

The role of GLDC in tumors appears to be tumor-type specific [12–14,20–22]. Aberrantly increased GLDC was detected in non-small cell lung cancer (NSCLC) and glioma [12,13]. Moreover, GLDC expression was significantly correlated with poor survival in NSCLC patients [12]. In these cancers, GLDC appears to be a metabolic oncogene and plays an important role in tumor initiation and proliferation, but in gastric cancer, GLDC was reported to be a putative tumor suppressor gene and hypermethylation of the GLDC promoter was detected in tumor tissues [14]. The role of GLDC in HCC is still unknown.

In this study, we sought to identify the enzymes in the glycine/serine pathway that are associated with HCC metastasis by using microarray-based analysis. GLDC expression was significantly decreased not only in two metastatic HCC cell lines, MHCC97L and HCCLM3, but also in HCC patient tissues. We investigated the role and the molecular mechanism by which the downregulation of GLDC promoted HCC metastasis.

2. Materials and methods

2.1. Reagents

Dulbecco's modified Eagle medium (DMEM), fetal bovine serum (FBS), penicillin, streptomycin, N-2-hydroxyethylpiperazine-N-2-ethane sulfonic acid (HEPES), Lipofectamine 2000, BCA reagents, Protein A and G magnetic beads were obtained from Invitrogen (Carlsbad, CA). Chemotaxis chambers and membranes were obtained from Neuroprobe (Gaithersburg, MD, USA). human epidermal growth factor (EGF) was from Peprotech (Rocky Hill, NJ, USA). Enhanced chemiluminescence (ECL) reagents were purchased from Pierce Biotechnology (Rockford, IL, USA). Protease Inhibitor Cocktail tablets were purchased from Roche Diagnostics (Indianapolis, IN, USA). Oregon Green 568 phalloidin from Molecular Probes Inc. (Eugene, OR). N-acetyl-L-cysteine (NAC), 2′,7′-Dichlorofluorescin diacetate (DCFH-DA) and MG132 were purchased from Sigma-Aldrich (Shanghai, China). cycloheximide (CHX) was purchased from Santa Cruz Biotechnology (CA, USA). H_2O_2 was purchased from Kermel (Tianjin, China).

2.2. Cell culture

The human HCC cell lines PLC, Hep3B and HepG2 were obtained from the American Type Culture Collection biobank. Huh7 was obtained from the Japanese Collection of Research Biosources. MHCC97L, MHCC97H and HCCLM3 were cultured as described [23,24]. BEL-7402 were obtained from Shanghai Institutes for Biological Sciences, Chinese Academy of Sciences. The cells were grown in DMEM with 10% FBS and 1% penicillin/streptomycin under 5% CO_2.

2.3. Clinical specimens

25 pairs of HCC tumor and para-tumor tissues were obtained from surgically resected samples from HCC patients in Affiliated Cancer Hospital of Zhengzhou University (Henan Cancer Hospital, Henan, China) with the informed consent of the patients and ethics approval from the Ethics Committee (No. 2016CT054) of Henan Cancer Hospital. The diagnosis of the liver samples was confirmed by pathology.

2.4. Generation of expression vector and stable transfection

Recombinant genes coding shRNA against GLDC and non-targeting shRNA (complete sequences were showed in Supplementary Table S1) were constructed to pLKO.1-TRC cloning vector (Addgene, Cambridge, MA, USA). Lentiviruses were produced and cells were transfected following the protocol online (http://www.addgene.org/plko). Stably transfected Huh7 and PLC cell lines were selected with 3 μg/ml and 1.5 μg/ml puromycin starting at 48 h after transfection respectively. GLDC cDNA clone was purchased from GenScript (Nanjing, China) and catalase-expressing plasmid was purchased from Sino Biological (Beijing, China). The knockdown and overexpression efficiency of GLDC were measured by Quantitative reverse transcription PCR (qRT-PCR) and Western blots.

2.5. RNA Extraction and qRT-PCR

Total RNA was extracted using TRIzol reagent (Invitrogen, CA) according to the manufacturer's instructions. Reverse transcription reactions were performed with 1 μg of total RNA using FastQuant RT kit (TIANGEN, Beijing, China). GLDC expression was quantified by SYBR qPCR Kit (TIANGEN, Beijing, China) according to the manufacturer's instructions. All samples were run in triplicate. 18s RNA was used as an endogenous RNA reference gene. The relative expression levels were evaluated using the $2^{-\Delta\Delta Ct}$ method [25]. Primers were listed in Supplementary Table S2.

2.6. Western blot analysis

The same amount of total cell lysates were prepared for Western blots as previously described [26]. Antibodies against cofilin (Abcam, Cambridge, UK); p-cofilin, β-actin (ImmunoWay Biotechnology, USA); HA monoclonal (Sigma); ubiquitin (Santa Cruz Biotechnology, CA, USA); SSH1, LIMK1/2, GLDC (Cell Signaling Technology, Beverly, USA) were used. The blots were subsequently developed by enhanced chemiluminescence (Millipore) using a horseradish peroxidase-conjugated secondary antibody (Santa Cruz).

2.7. Wound healing, chemotaxis, migration, and invasion assays

For the wound healing assays, the cells were plated in 6-well plates for 2 days to grow a mono-layer, and then they were pretreated with serum-free DMEM for 12 h. After which, a linear scratch was made in the middle using a 10-μl pipette tip. The cells were then cultured in DMEM with 2% FBS at 37 °C in 5% CO_2, and the wound widths were measured with a microscope at different time points and photographed at the beginning and the end of the observation, respectively.

The chemotaxis assay was conducted using micro-Boyden chambers as described by Sun et al. [27]. Briefly, different concentrations of EGF (0, 1, 10, and 100 ng/ml) were loaded into the lower chamber and then cells (5×10^5 cells/ml) were suspended in binding medium (DMEM, 0.1% bovine serum albumin (BSA, Solarbio, Beijing, China), and 25 mM HEPES) and loaded into the upper chambers. After incubating for 6 h, the filter membrane was washed, fixed, and then stained. The number of migrating cells was counted microscopically.

Migration and invasion assays were performed using 24-well Transwell chambers containing polycarbonate membranes with 8-μm pores (Corning, Tewksbury MA, USA). For the invasion assays, the membrane was coated with Matrigel (BD Biosciences, San Jose, CA, USA). Serum-starved cells were added to the upper chamber and incubated in serum-free medium. Then, 600 μl DMEM with 10% FBS was

added to the lower chamber. After that Huh7 and PLC cells were incubated for 20 h, while HCCLM3 and MHCC97L cells were incubated for 12 h at 37 °C, respectively. After that, non-migration or non-invasive cells on the upper membrane surface were removed with a cotton swab, while the migration and invasive cells on the under-surface were fixed and stained. The number of migration and invasive cells were counted microscopically.

2.8. Staining of cytoskeletal components

Cells were seeded in 24-well plates containing sterile coverslips and cultured for 48 h. Cells were fixed in 4% paraformaldehyde (Solarbio, Beijing, China) for 10 min at room temperature (RT), permeabilized with 0.1% Triton X-100 for 5 min, and then washed three times with PBS. Blocking of unspecific binding sites was performed by incubation in 1% BSA in PBS for 60 min at RT. Then cells were incubated with Rhodamine conjugated phalloidin (Cytoskeleton, USA) for 30 min at 37 °C, followed by incubation with 1 μg/ml of 4,6′-diamidino-2-phenylindole (DAPI) (1:5000 dilution, ZhongShan Goldenbridge, Beijing, China) for 10 min at RT. Morphological features were quantified using a confocal laser scanning microscopy (Olympus FV1000).

2.9. ROS detection

Fluorescent dye, DCFH-DA was used to determine the intracellular ROS levels. Cells were harvested and washed with PBS and then exposed to 10 mM DCFH-DA at 37 °C for 30 min. ROS levels were analyzed by flow cytometry using Becton Dickinson's FACScan. In the immunofluorescence assays, the cells were seeded on sterile coverslips in 24-well plates at no more than 50% confluence after a 24-h growth period and starved in serum-free medium overnight. After incubation with 50 mM DCFH-DA for 10 min at 37 °C, the cells were fixed with 4% paraformaldehyde. DAPI was stained as described above. Coverslips were mounted and visualized with confocal laser scanning microscopy (Olympus FV1000, Japan).

2.10. Glutathione measurement

The cellular glutathione levels were measured by GSH/GSSG Ratio Detection Assay (Abcam, Cambridge, UK) and a deproteinizing sample preparation kit-TCA (Abcam) according to the manufacturer's protocol.

2.11. Ubiquitin ladder assay

Cell lysates were prepared by incubating cells in 1% Tris-Triton cell lysis buffer (Cell Signaling Technology, Danvers, MA, USA) containing 1 mM PMSF and protease inhibitor cocktail on ice for 30 min, after which the lysates were centrifuged at 12,000 × *g* for 15 min. The supernatants were incubated overnight with 30 μl Dynabeads Protein A (Life Technologies, USA) precoated with anti-cofilin (Abcam, Cambridge, UK), or anti-ubiquitin (Proteintech, Wuhan, China) antibodies. The immunocomplexes were analyzed by Western blots. A normal IgG control was assayed simultaneously.

2.12. In vivo metastasis assays

5-week-old male BALB/c-nude mice (Chinese Academy of Sciences, Beijing, China) were used for the intrahepatic metastasis assays [28]. Briefly, 2×10^6 cells were suspended in 20 μl of serum-free DMEM and 20 μl of Matrigel for each mouse (n = 6 mice for each cell line). Through an 8-mm midline incision in the upper abdomen under anesthesia, cells were orthotopically inoculated in the left hepatic lobe by a microsyringe. After 6 weeks, mice were sacrificed, and their livers were dissected, and fixed with 4% paraformaldehyde for following standard histological examination. The experimental protocols were evaluated and approved by Tianjin Medical University Animal Care and Use Committee.

2.13. Haematoxylin and eosin (H&E) and Immunohistochemistry (IHC) staining

All of the tissue samples were fixed in paraformaldehyde for 24 h, embedded in paraffin (Leica Biosystems, Richmond, USA), and then cut into 4 μm-thick sections. For H&E staining, the tissue sections were deparaffinized, rehydrated and stained with an H&E staining kit (Beyotime Institute of Biology, Suzhou, China). For IHC staining, the sections were dried at 60 °C for 2 h and then deparaffinized with 3 washes of xylene for 5 min each. The sections were rehydrated in graded alcohols, followed by incubating in 3% hydrogen peroxide for 30 min. For antigen retrieval, the sections were boiled in 10 mM citrate buffer, pH 6.0. Next, the slides were incubated overnight at 4 °C with cofilin antibody diluted at 1:50 in 1% BSA solution. The primary antibodies were detected with the Polink-1 HRP DAB detection system (ZSGB-Bio, Beijing, China) to assess the histology and morphology of intrahepatic metastasis in the mouse models.

2.14. Bioinformatic and statistical analysis

The cBioPortal online software (http://www.cbioportal.org/) was used for the clinical HCC data obtained from The Cancer Genome Atlas (TCGA) [29]. We analyzed the data from 2000 to 2013, and a total of 203 cases of HCC patients with GLDC mRNA expression data and complete follow-up information were enrolled in this study. Based on the GLDC expression, overall survival (OS) was calculated by Kaplan-Meier survival analysis and log-rank tests. Clinicopathological correlations were analyzed by Pearson's *chi*-square test. Student′s *t*-test was used for comparison between two groups and one-way analysis of variance (ANOVA) was performed among multiple groups. Data were presented as mean ± S.D. Statistical Product and Service Solutions (SPSS) version 17.0 software was used for all of the data analyses and $P < 0.05$ was considered to be a significant difference.

3. Results

3.1. HCC tumors express lower GLDC

To identify the enzymes in the glycine/serine pathway that are associated with HCC malignancy, we analyzed the microarray data (Gene Expression Omnibus No. GSE97626) on three HCC cell lines with increasing metastatic potential, Huh7, MHCC97L, and HCCLM3 [23,24,30]. Among the 17 enzymes involved in glycine metabolism that are listed in the Kyoto Encyclopedia of Genes and Genomes (KEGG) database [13], we found that GLDC expression (Agilent Probe ID: agiseq. 6111, Accession: NM_000170.2) was significantly reduced in the highly malignant MHCC97L and HCCLM3 cells, in comparison to the Huh7 cells (Fig. 1A). qRT-PCR confirmed the reduction of GLDC in the MHCC97L and HCCLM3 cells (Fig. 1B). Western blot analysis also confirmed the low expression of GLDC in highly malignant HCC cells, and this was supported by the qRT-PCR results (Supplemental Fig. S1).

Next, GLDC expression was examined in the samples from 25 HCC patients (Supplementary Table S3). qRT-PCR showed that the GLDC expression was significantly downregulated in the HCC tumor tissues compared with that of the corresponding adjacent benign tissues (Fig. 1C). We selected 7 patient samples for Western blot analysis, and the results showed a decrease in the GLDC protein levels in the tumor tissues (Fig. 1D). We then analyzed the clinicopathological information of the GLDC expression from TCGA. Statistical analyses revealed that GLDC downregulation was significantly associated with advanced the American Journal of Critical Care (AJCC) staging (Supplementary Table S4, $X^2 = 6.283$, $P = 0.043$). In addition, Kaplan-Meier survival analysis revealed that GLDC downregulation correlated with shorter OS in HCC patients (Fig. 1E, $P < 0.05$). Taken together, our results suggest that

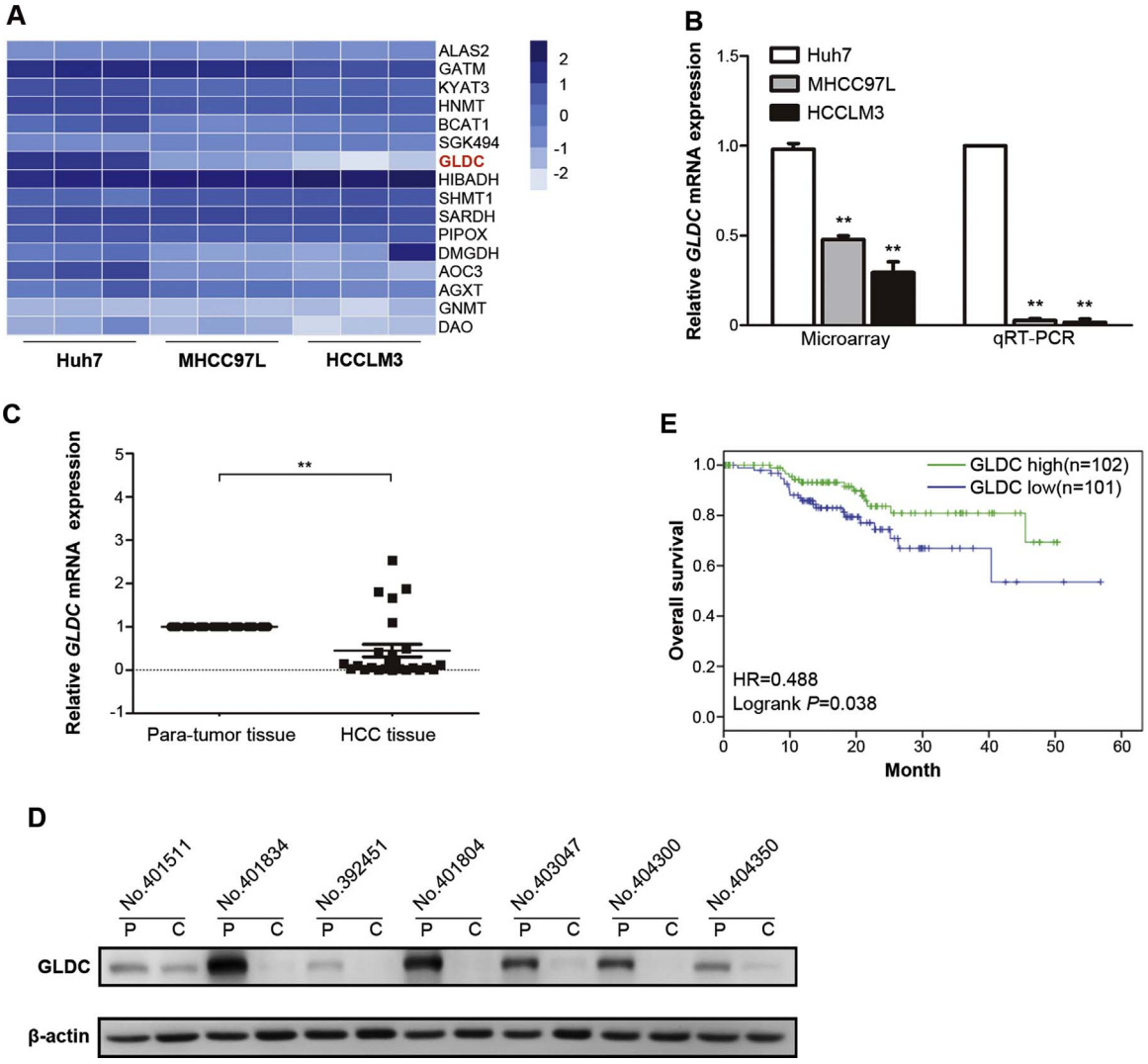

Fig. 1. GLDC downregulation is associated with HCC metastasis. (A) Differentially expressed enzymes related with glycine/serine pathway in different metastatic potential HCC cell lines (Huh7, MHCC97L, and HCCLM3) in microarray. (B) GLDC mRNA levels detected by qRT-PCR analysis compared with those detected by microarray. (C) qRT-PCR analysis of GLDC mRNA levels in 25 pairs of HCC tumor tissues and para-tumor tissues. (D) Western blot analysis of GLDC expression in selected 7 pairs of HCC tissues and para-tumor tissues. (E) Kaplan-Meier analysis of overall survival of patients from the TCGA database stratified by GLDC mRNA expression ($P = 0.038$, logrank tests). Bar: mean; error bars: S.D.; $^{**}P < 0.005$; HR, hazard ratio; P, para-tumor tissues; C, HCC tissues.

GLDC is downregulated in HCC tumors and its decreased levels appears to be correlated with a poor survival rate.

3.2. Decrease in GLDC promotes HCC migration and invasiveness in vitro

To investigate the functional significance of GLDC in HCC metastasis, GLDC was knocked down in the Huh7 and PLC cells, and overexpressed in the HCCLM3 and MHCC97L cells (Supplemental Fig. S2). A wound healing assay showed that GLDC knockdown significantly promoted cell migration in the Huh7 and PLC cells, while GLDC overexpression impaired cell migration in the HCCLM3 and MHCC97L cells (Fig. 2A and B). In the Transwell chamber and Matrigel invasion assays, GLDC knockdown significantly enhanced the migration and invasiveness while overexpression inhibited them (Fig. 2C and D). EGF-induced chemotaxis was also enhanced in the GLDC-knockdown cells and impaired in the GLDC-overexpressing cells (Fig. 2E and F). Taken together, the results show that GLDC downregulation promotes HCC cell migration and invasiveness.

3.3. Decrease in GLDC enhances actin polymerization via increasing protein levels of cofilin

Actin polymerization is a key step during cell locomotion [31]. As shown in confocal fluorescence microscopy, GLDC knockdown led to the enrichment of filamental actin (F-actin) on cell membranes and an increase in lamellipodium, which is consistent with increased cell migration (Fig. 3A). GLDC overexpression dampened the levels of membrane F-actin (Fig. 3B). Thus, GLDC levels appear to modulate cytoskeleton rearrangement and lamellipodium formation.

Cofilin is able to bind to F-actin, which contributes to F-actin severing and depolymerization; this is inhibited by its phosphorylation (p-cofilin) [32]. Western blot analysis showed that total cofilin expression was upregulated with GLDC knockdown in the Huh7 and PLC cells (Fig. 3C) and downregulated with GLDC overexpression in the HCCLM3 and MHCC97L cells (Fig. 3D). Meanwhile, the protein levels of p-cofilin were significantly decreased in the GLDC-knockdown cells and increased with GLDC overexpression compared to the corresponding control cells (Fig. 3C and D). Cofilin activity is tightly controlled by LIM kinase 1/2 (LIMK 1/2), which phosphorylates cofilin at Ser-3. Accordingly, dephosphorylation by the phosphatase slingshot homolog 1

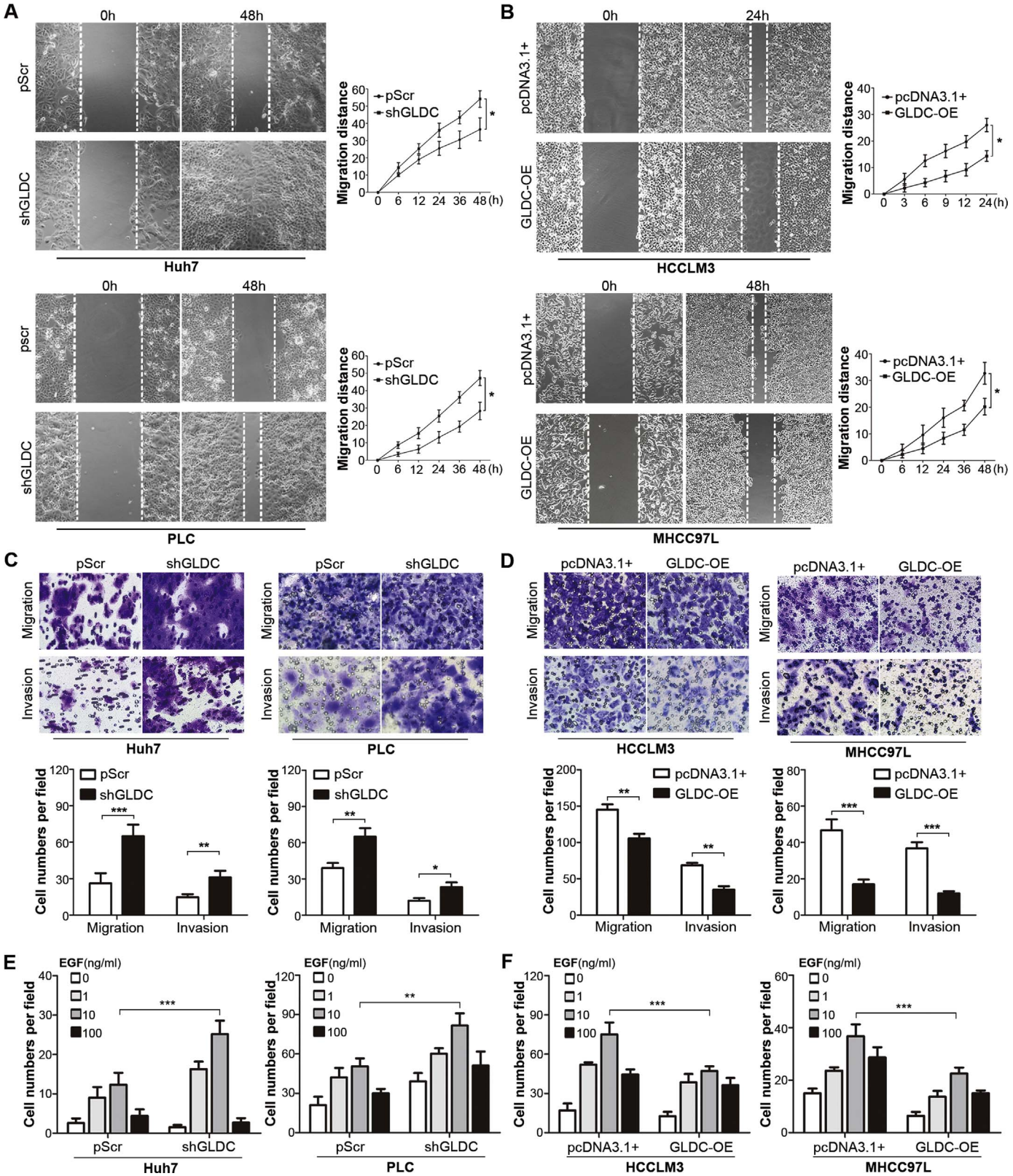

Fig. 2. GLDC inhibits HCC cells migration and invasiveness in vitro. (A-B) Wound-healing assays using GLDC-knockdown and GLDC-overexpressing cells. Representative images at 0 h and 24 h or 48 h (left panel), magnification: 100 × . Line graph showing migration values at 3-h, 6-h, or 12-h intervals (right panel). (C-D) Transwell-chamber assays and Matrigel invasion assays using GLDC-knockdown and GLDC-overexpressing cells. Representative images of the migratory or invading cells (upper panel), magnification: 400 × . Histogram of the numbers of migratory or invading cells (below panel). (E-F) Chemotaxis analysis using GLDC-knockdown and GLDC-overexpressing cells with different doses of EGF. The results shown are the representatives of at least two independent experiments. Bar: mean; error bars: S.D.; $^{*}P < 0.05$, $^{**}P < 0.005$, $^{***}P < 0.0005$.

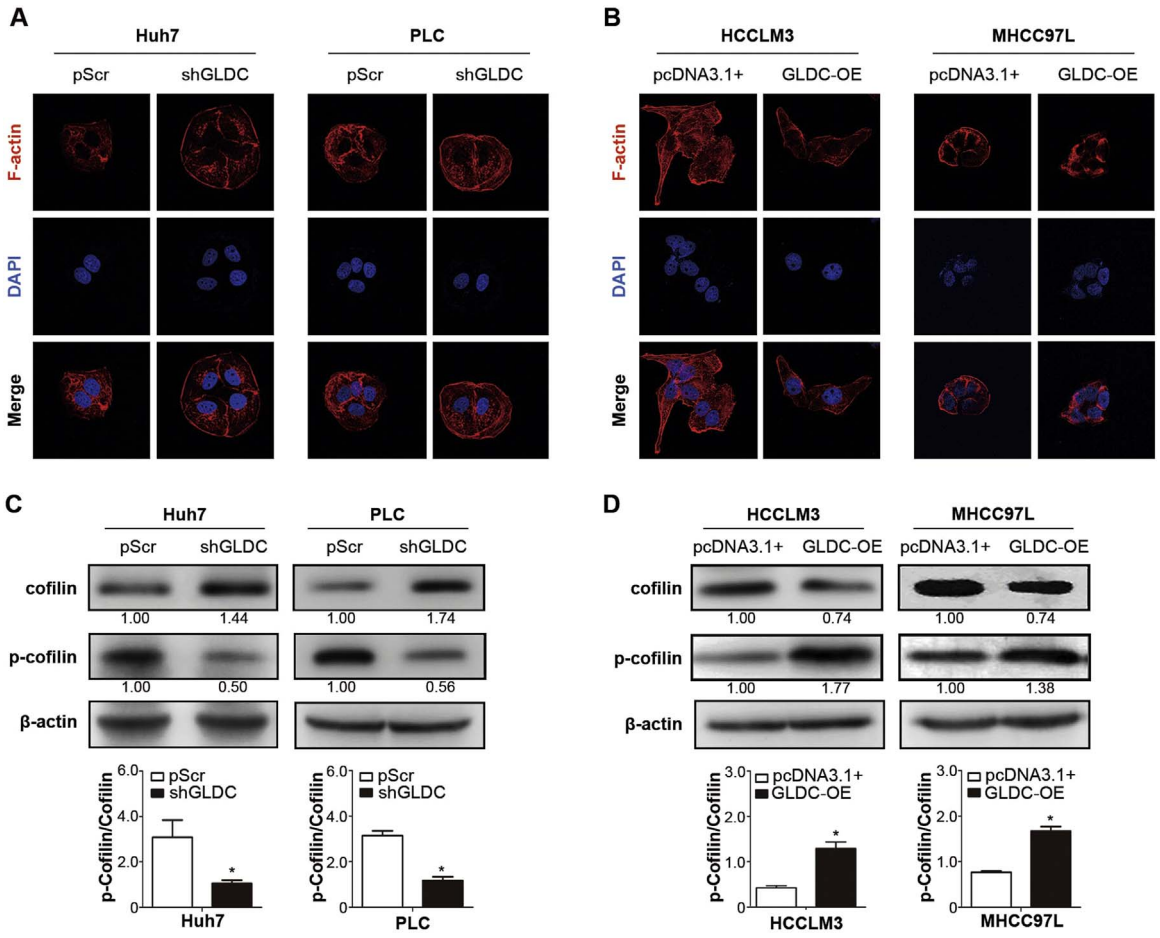

Fig. 3. GLDC decrease enhances actin polymerization via increasing protein levels of cofilin. (A-B) Immunofluorescence analysis of F-actin levels using GLDC-knockdown and GLDC-overexpressing cells. (C-D) Western blot analysis of cofilin and p-cofilin expression levels in GLDC-knockdown and GLDC-overexpressing cells. Histogram showed the relative intensity of cofilin phosphorylation verses total cofilin levels in GLDC-knockdown and GLDC-overexpressing cells. Data represent the means ± SD of triplicate independent experiments (*$P < 0.05$, by student's *t*-test).

(SSH1) reactivates cofilin [33,34]. As shown in Supplemental Fig. S3, Western blot analysis showed that SSH1 expression was upregulated in the GLDC-knockdown cells and downregulated in the GLDC-overexpressing cells. We did not detect any change in LIMK1/2 expression. The results indicate that with GLDC knockdown, the decrease of p-cofilin might be enhanced by increased SSH1 levels, which then cause the cytoskeleton rearrangement and alter the behavior of HCC cells.

Meanwhile, mRNA levels of cofilin were examined using qRT-PCR. The results showed that neither GLDC knockdown nor GLDC overexpression altered the mRNA levels of cofilin (Supplemental Fig. S4), suggesting that GLDC might regulate cofilin protein levels through a post-transcriptional mechanism. Taken together, the results reveal that GLDC downregulation elevates the protein levels of cofilin and decreases the cofilin phosphorylation level which may directly promote cell migration.

3.4. Knockdown of GLDC impairs cofilin ubiquitination associated with ROS elevation

We tested the hypothesis that GLDC might regulate cofilin protein stability. As shown in Fig. 4A, treatment with CHX at 10 μg/ml, a potent inhibitor of protein translation, decreased the levels of cofilin, probably due to protein degradation. Cofilin degradation was significantly impaired in the GLDC-knockdown cells, suggesting that GLDC might be involved in cofilin degradation. Treatment with MG132 at 10 μM, a proteasomal inhibitor, rescued GLDC-induced decrease in cofilin levels, and further confirmed the role of GLDC in cofilin degradation (Fig. 4B). The proteasome-mediated degradation of ubiquitinated proteins is a main pathway to regulate the expression of various proteins in cells [35]. Western blot analysis showed a reduced ubiquitination of endogenous cofilin in the GLDC-knockdown cells compared with the corresponding control cells (Fig. 4C). These results suggest GLDC knockdown inhibits cofilin degradation through the ubiquitin-proteasome pathway.

Glycine is a building block of glutathione [36]. It has been reported that the ratio of the reduced versus oxidized form of glutathione (GSH/GSSG) regulates the levels of endogenous ubiquitin-activating enzyme (E1)-ubiquitin thiol esters, which in turn regulates protein degradation [37,38]. We first detected the total GSH&GSSG level and found it was increased in the GLDC-knockdown cells compared with its corresponding control cells, which is consistent with a previous report [11] (Fig. 4D). Then we found that the relative GSH/GSSG ratio was decreased in the GLDC-knockdown cells (Fig. 4E). Consequently, the intracellular total protein-ubiquitin conjugates appeared to be decreased in the GLDC-knockdown cells (Fig. 4F).

The GSH/GSSG ratio plays an important role in tumor cell survival and it is reported to decrease in the presence of oxidative stress [39]. We used DCFH-DA as a probe to examine the intracellular levels of ROS. As shown by confocal fluorescence microscopy and flow cytometry analyses, GLDC knockdown significantly increased the ROS levels, whereas GLDC overexpression reduced it (Fig. 4G-J). Taken together, the results show that GLDC knockdown appears to increase cellular ROS levels, decrease the GSH/GSSG ratio, and enhance cellular protein ubiquitination, including cofilin, which may account for the elevated

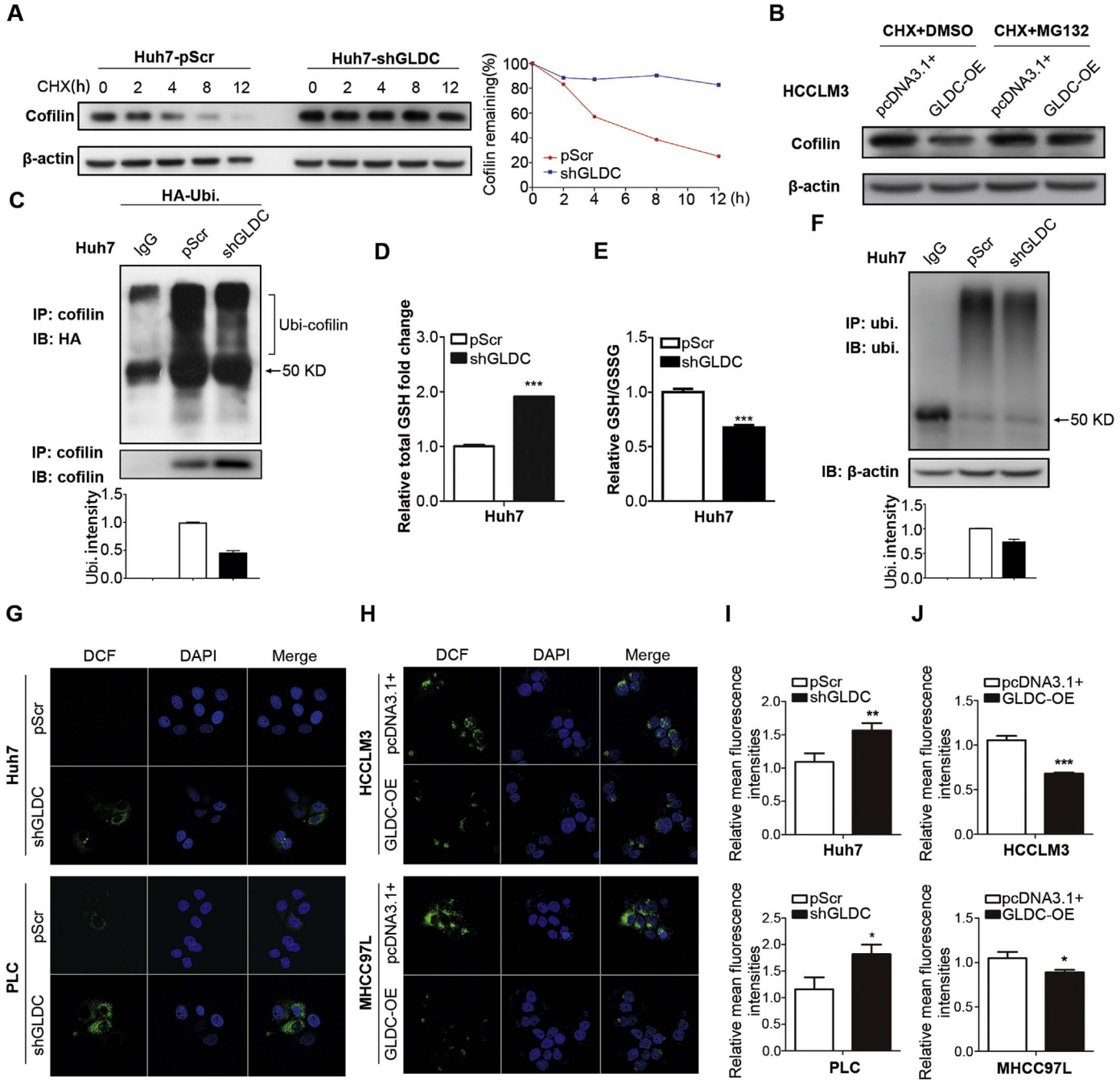

Fig. 4. GLDC knockdown impairs cofilin ubiquitination associated with ROS elevation. (A) GLDC-knockdown cells and its corresponding control cells were incubated with 10 μg/ml of CHX, and cell lysates were generated at the indicated time points (hours) respectively. Cofilin expression levels were detected by Western blots (left panel) and quantified by densitometer. The line graph shows the relative intensity of cofilin verses β-actin (right panel). (B) GLDC-knockdown cells and its corresponding control cells were incubated with 10 μg/ml of CHX either in the presence or in the absence of 10 μM MG132. Cofilin expression levels were detected by Western blots. (C) After transfected with HA-Ubi-overexpressing plasmid, the lysates of GLDC-knockdown cells and its control cells were prepared and immunoprecipitated with anti-cofilin antibody, followed by Western blots with anti-HA (upper) or anti-cofilin (lower). The ubiquitinated cofilin bands are marked on the right. (D-E) Assays for GSH and GSSG by a GSH/GSSG Ratio Detection Assay kit and a deproteinizing sample preparation kit-TCA (Abcam) using GLDC-knockdown cells and its control cells. (F) The lysates of GLDC-knockdown cells and its control cells were prepared and immunoprecipitated with anti-ubiquitin antibody, followed by Western blot with anti-ubiquitin (upper) or anti-β-actin (lower). (G-J) Intracellular ROS production determined after incubation with 10 μM of DCFH-DA. (G-H) Representative confocal images of GLDC-knockdown cells and GLDC-overexpressing cells. The cell nuclei were stained with DAPI (blue fluorescence). (I-J) Flow cytometry-measured relative mean fluorescence intensities of intercellular DCFH-DA in GLDC-knockdown cells and GLDC-overexpressing cells. Bar: mean; error bars: S.D.; $^{*}P < 0.05$, $^{**}P < 0.005$, $^{***}P < 0.0005$.

cell migration of HCC cells.

3.5. Oxidative stress inhibits cofilin degradation in GLDC-knockdown cells

To confirm the hypothesis that GLDC regulated cofilin degradation through modulating oxidative stress, we first used NAC, a major thiol-related antioxidant and ROS scavenger [40], to rescue the phenotype of GLDC-knockdown cells. Western blot analysis showed that NAC restored not only cofilin degradation in a dose-dependent manner, but also cofilin ubiquitination in GLDC-knockdown cells (Fig. 5A and Supplemental Fig. S5). The relative GSH/GSSG ratio was also rescued by NAC in GLDC-knockdown cells (Fig. 5B). The results of the Transwell

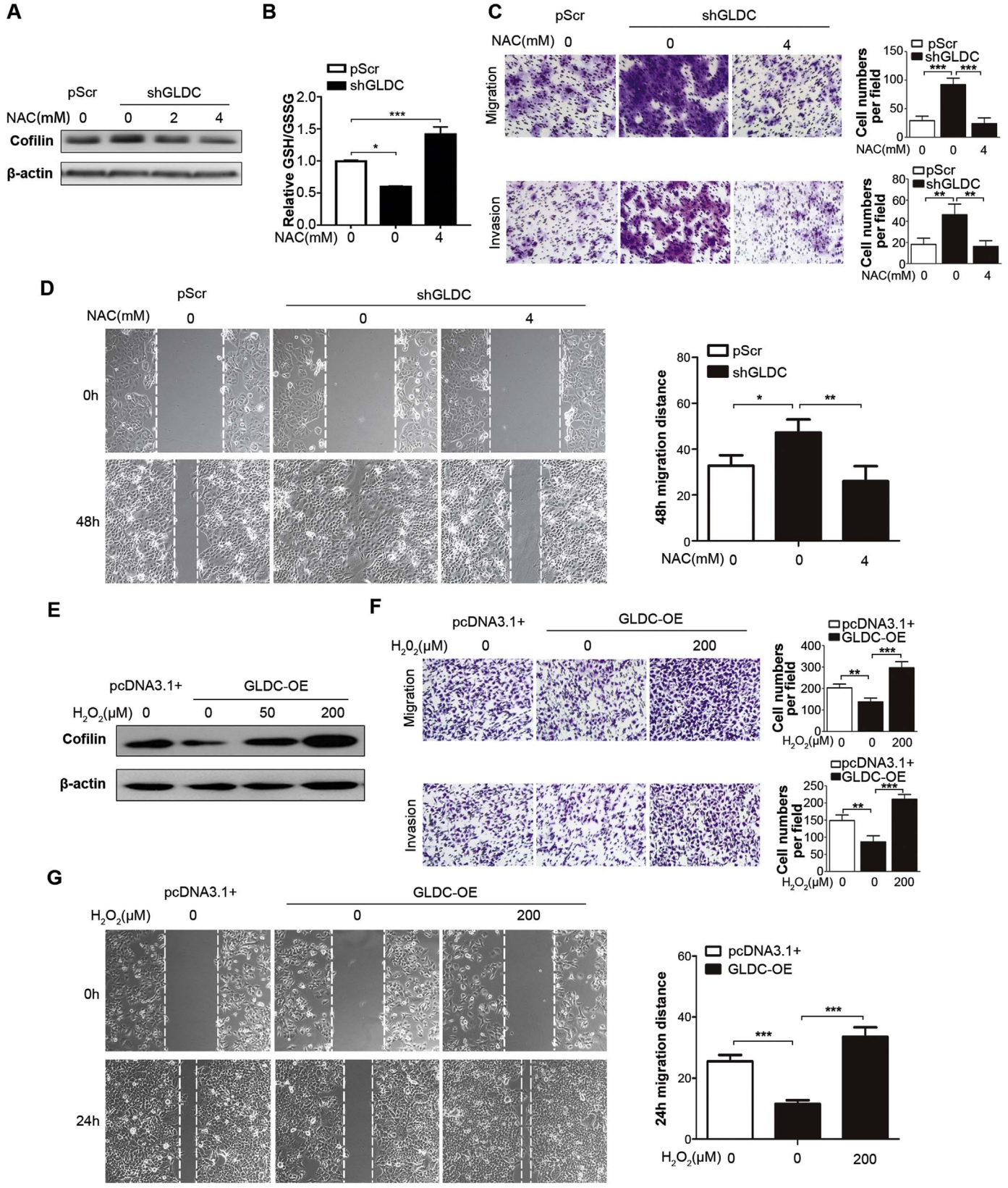

Fig. 5. Oxidative stress inhibits cofilin degradation in GLDC-knockdown cells. (A) GLDC-knockdown Huh7 cells and its control cells were pretreated with or without indicated concentration of NAC for 12 h. Cofilin expression levels were detected by Western blots. (B) Histogram showing relative ratios of GSH/GSSG. (C-D) Transwell-chamber assays, Matrigel invasion assays, and wound-healing assays using GLDC-knockdown Huh7 cells and its control cells either in the presence or in the absence of 4 mM NAC, magnification: 100 × . (E) GLDC-overexpressing HCCLM3 cells and its control cells were pretreated with or without indicated concentration of H_2O_2 for 12 h. Cofilin expression levels were detected by Western blots. (F-G) Transwell-chamber assays, Matrigel invasion assays, and wound-healing assays using GLDC-overexpressing HCCLM3 cells and its control cells either in the presence or in the absence of 200 μM H_2O_2, magnification: 100 × . Bar: mean; error bars: S.D.; $^{*}P < 0.05$, $^{**}P < 0.005$, $^{***}P < 0.0005$.

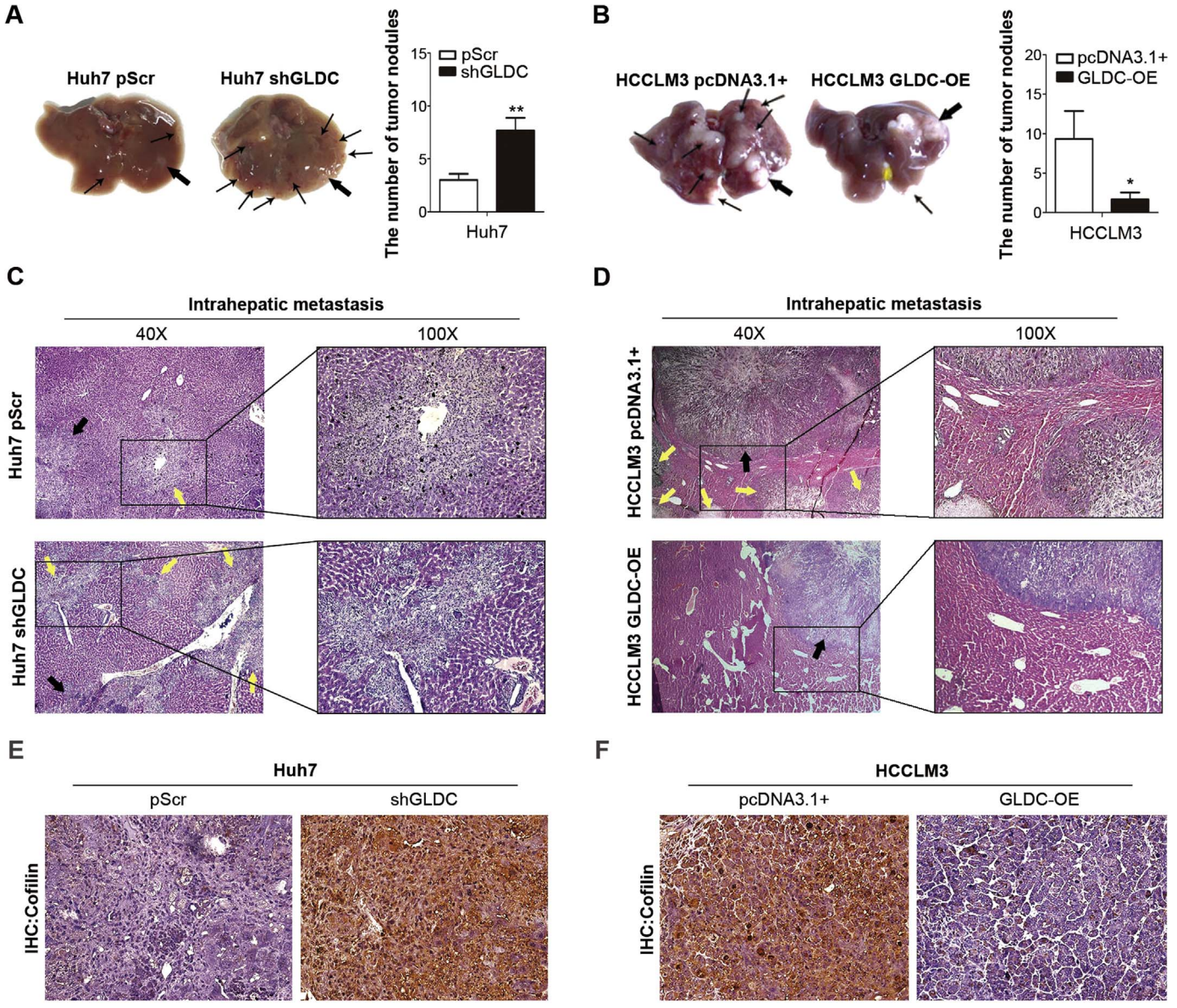

Fig. 6. GLDC inhibits intrahepatic metastasis in an orthotopic mouse model. (A-B) Representative images showing the intrahepatic metastases (marked with thin black arrows) and the orthotopic transplanted tumor (marked with bold black arrows) in the orthotopic mouse models transplanted with GLDC-knockdown Huh7 cells or GLDC-overexpressing HCCLM3 cells and their corresponding control cells. The surface tumor nodules were counted and plotted (n = 6, $*P < 0.05$, $**P < 0.005$.). (C-D) Histologic analyses of orthotopic primary liver tumors (black arrows) and intrahepatic metastatic nodules (yellow arrows) in the orthotopic mouse models transplanted with GLDC-knockdown Huh7 cells or GLDC-overexpressing HCCLM3 cells and their corresponding control cells. (E-F) Representative IHC images of cofilin expression in tumor xenografts in the orthotopic mouse models transplanted with GLDC-knockdown Huh7 cells or GLDC-overexpressing HCCLM3 cells and their corresponding control cells, magnification: 200 × .

chamber assays and the Matrigel invasion assays showed that the treatment with NAC at 4 mM blocked cell migration and invasion induced by GLDC knockdown (Fig. 5C). Wound healing assays further confirmed that NAC treatments rescued the phenotype of the GLDC-knockdown cells (Fig. 5D). Catalase, which catalyzes the decomposition of H_2O_2 [41], was also used to rescue the phenotype of GLDC-knockdown cells by transient transfection of catalase-expressing plasmid. The results showed that catalase overexpression reversed the reduction in cofilin ubiquitination, and promoted cell migration and invasion in response to the GLDC downregulation (Supplemental Fig. S6).

We then tested our hypothesis by treatment with H_2O_2, which elevated cellular oxidative stress. The repression of cofilin ubiquitination was lost in the GLDC-overexpressing cells after treatment with H_2O_2 for 12 h (Fig. 5E). Moreover, the decreased ability to migrate and invade induced by GLDC overexpression was rescued upon H_2O_2 treatments (Fig. 5F). And wound-healing assays further confirmed that H_2O_2 treatments blocked the phenotype of the GLDC-overexpressing cells (Fig. 5G). Taken together, our results further suggest that oxidative stress regulates cofilin degradation.

3.6. GLDC Knockdown promotes intrahepatic metastasis in vivo

To determine the metastatic relevance of GLDC in vivo, we examined the effect of GLDC in an orthotopic HCC mouse model. The Huh7 cells are low metastatic HCC cells. In 6 nude mice, GLDC-knockdown Huh7 cells showed a significant increase in intrahepatic metastasis (Fig. 6A). HCCLM3 cells are highly metastatic HCC cells. In 6 nude mice, GLDC overexpression significantly decreased intrahepatic metastasis of HCCLM3 cells (Fig. 6B). Histologic analyses of mouse liver tissues further confirmed the role of GLDC in intrahepatic metastases (Fig. 6C and D). Moreover, cofilin expression was increased in the mice transplanted with the GLDC-knockdown Huh7 cells and downregulated

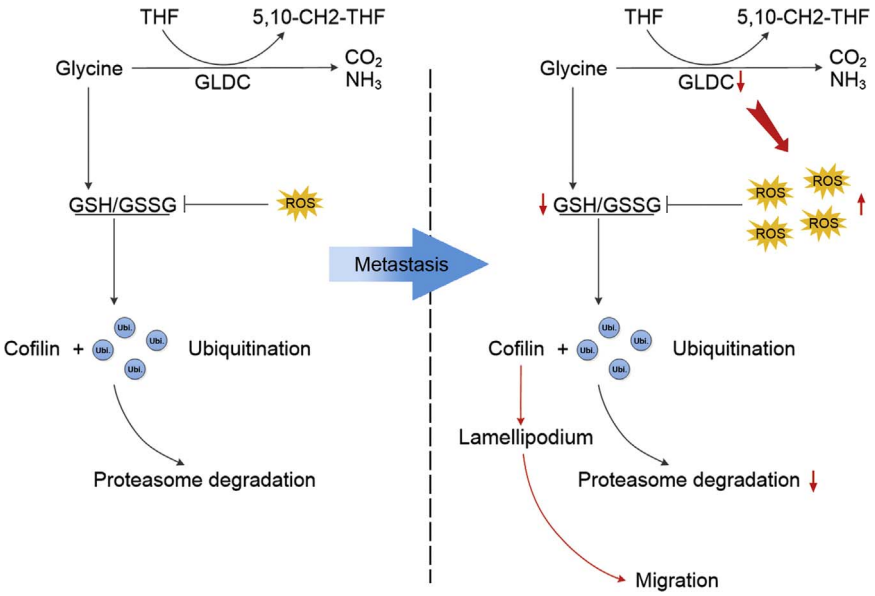

Fig. 7. Diagram of GLDC-mediated activation of cofilin ubiquitination by inhibiting redox stress to oppose HCC migration.

in the mice transplanted with the GLDC-overexpressing HCCLM3 cells in comparison to those transplanted with their corresponding control cells (Fig. 6E and F). These results further confirm that GLDC dysregulation plays an important role in HCC metastasis.

4. Discussion

Metabolic reprogramming is a hallmark of cancer [7]. Recent reports have started to reveal that the dysregulation of amino acid metabolism is not merely a consequence of tumorigenesis, but it is actively involved in tumor progression and metastasis [8,9]. Our results showed an important role of GLDC, an oxidoreductase, in HCC invasion and metastasis. In a microarray study, we found that GLDC expression was significantly decreased in the highly metastatic HCC cell lines, MHCC97L and HCCLM3. qRT-PCR analysis of 25 HCC patient tissues showed that the GLDC levels were significantly lower in the HCC tissues. A decrease in GLDC expression appeared to be linked with advanced HCC tumor staging and a poor patient survival rate. GLDC knockdown enhanced HCC cell migration, invasion, and metastasis while GLDC overexpression reversed the phenotype. Therefore, our results clearly indicated that GLDC regulated HCC migration and metastasis in a reciprocal manner.

It has been well documented that tumor cells acquire a more aggressive phenotype under oxidative stress [42,43]. Previous studies have shown that cofilin, the key regulator of F-actin depolymerization, controls actin dynamics and is redox sensitive [44]. Cofilin activation is modulated by ROS both directly and indirectly and cofilin is a target for oxidation. H_2O_2 mediates redox-dependent dephosphorylation of cofilin in human vascular smooth muscle cells [45]. The oxidation of cofilin cysteine residues with taurine chloramine treatments loses the ability of cofilin to bind F-actin and induces apoptosis [46]. In addition, ROS could be generated at the leading edge of a migrated MDAMB231 breast cancer cell resulting in oxidations on Cys139 and Cys147 in cofilin and blocking actin-cofilin binding, thus promoting directional motility [47]. On the other aspect, SSH-1, a cofilin regulatory phosphatase, is activated by ROS, which is stimulated by angiotensin II, to dephosphorylate cofilin [48]. Further, Mical, an actin-oxidizing enzyme, combines with cofilin to form a redox-dependent synergism that magnifies the effects of both Mical and cofilin on actin filament dismantling [49]. Our results showed that GLDC downregulation enhances the levels of ROS and promoted cell migration, which was consisted with previous reports [42,43].

Of note, we revealed a novel mechanism in this study by which cofilin is stabilized under oxidative stress. There are clues on the connection of oxidation with ubiquitination and phosphorylation [50]. A previous study showed that cofilin phosphorylation triggers its degradation via ubiquitin-proteasome pathway [35]. A lower ratio of GSH/GSSG promotes glutathionylation of cellular proteins. S-glutathionylation of cofilin have been recognized after cells are exposed to oxidants [51,52]. However, the relationship between phosphorylation and glutathionylation of cofilin induced by ROS has not been reported. SSH-1 is activated upon its dissociation from its regulatory protein, 14–3-3ζ. Hyper-S-glutathionylation and degradation of 14–3-3ζ under oxidative stress are the key steps for SSH-1 release contributing to dephosphorylation of cofilin [53]. Here, we reported that GLDC regulated ROS levels in HCC cells. GLDC knockdown enhanced ROS levels while GLDC overexpression lowered it. It is reasonable to assume that S-glutathionylation indirectly enhances the stability of cofilin. In addition, a decreased ratio of GSH/GSSG is associated with a concomitant decrease in activity of the ubiquitinylation pathway upon oxidative stress [37]. The active sites of the E1 ubiquitin-activating enzyme, E2-ubiquitin conjugating enzyme, some E3 enzymes, and the deubiquitinases all have cysteine residues, which are sensitive to ROS [54]. The rapid increase of GSSG and the depletion of GSH contributes to the oxidation of these cysteine resides and the generation of mixed disulfide bonds, resulting in blocking their binding to ubiquitin [37]. Based on our results, we propose the following model in HCC (Fig. 7). The downregulation of GLDC enhances the levels of ROS and decreases the ratio of GSH/GSSG, which in turn reduces the ubiquitination of cofilin and promotes HCC invasion and metastasis. Consequently, the GLDC-knockdown cells showed impaired ubiquitination and elevated protein levels of cofilin. Thus, except for cofilin phosphorylation affected by ROS, the protein stability of cofilin appeared to be an important target of ROS-enhanced cell migration. Further investigation is needed to be elucidated the detailed post-translation regulation mechanism of cofilin under redox stress.

The expression of GLDC appears to be tumor type specific. In NSCLC, high expression of GLDC promotes cell proliferation, probably through enhanced serine levels, which activates PKM2 [12]. Decrease in GLDC levels were detected in gastric and liver cancers, suggesting that high level of GLDC is not required for the proliferation of these cancer cells [14]. It is possible that hepatocellular carcinoma can effectively use mitochondrial oxidative phosphorylation to generate ATP under limited activity of glycolysis and survive. The increase in ROS

production in GLDC down-regulated cells presumably reflects the increase in mitochondrial activity. Consequently, a decrease in GSH/GSSG contributes to elevated cell migration.

In summary, our results further confirm the importance to target oxidative stress during cancer therapy. However, we also notice that metabolism is a vast and complicated network. For example, the serine/glycine pathway is complexly intertwined with generation of intermediates for one-carbon metabolism, which is also associated with human cancers [55]. Measurements of both the rate and directionality of flux are important and need further exploration. In addition, although GLDC plays an important role in various tumors, we need to carefully consider its unique role in different tumors.

Acknowledgments

This work was supported by 863 Program [2015AA020403], National Key Research and Development Program [2016YFC0900100], Natural Science Foundation of China [21575103, 31671421, 81472683], NSFC-FRQS Program [81661128009], National Key Scientific Instrument and Equipment Development Project [2013YQ16055106], Science and Technology Development Foundation of Henan Province [172102310103, 152300410162], National Student's Platform for Innovation and Entrepreneurship Training Program [201710062002]. Tianjin Science and Technology Major Projects and Programs for “Precise Medical Major Project” [15ZXJZSY00030]. We would like to thank LetPub (www.letpub.com) for providing linguistic assistance during the revision of this manuscript.

Conflicts of interest

None.

Appendix A. Supporting information

Supplementary data associated with this article can be found in the online version at http://dx.doi.org/10.1016/j.freeradbiomed.2018.03.003.

References

[1] J. Ferlay, I. Soerjomataram, R. Dikshit, S. Eser, C. Mathers, M. Rebelo, D.M. Parkin, D. Forman, F. Bray, Cancer incidence and mortality worldwide: sources, methods and major patterns in GLOBOCAN 2012, Int. J. Cancer 136 (5) (2015) E359–E386.
[2] S.F. Altekruse, K.A. McGlynn, M.E. Reichman, Hepatocellular carcinoma incidence, mortality, and survival trends in the United States from 1975 to 2005, J. Clin. Oncol. 27 (9) (2009) 1485–1491.
[3] R. Xue, J. Li, F. Bai, X. Wang, J. Ji, Y. Lu, A race to uncover a panoramic view of primary liver cancer, Cancer Biol. Med. 14 (4) (2017) 335–340.
[4] A. Forner, A.J. Hessheimer, M. Isabel Real, J. Bruix, Treatment of hepatocellular carcinoma, Crit. Rev. Oncol. Hematol. 60 (2) (2006) 89–98.
[5] I.J. Fidler, The pathogenesis of cancer metastasis: the 'seed and soil' hypothesis revisited, Nat. Rev. Cancer 3 (6) (2003) 453–458.
[6] S. Katyal, J.H. Oliver 3rd, M.S. Peterson, J.V. Ferris, B.S. Carr, R.L. Baron, Extrahepatic metastases of hepatocellular carcinoma, Radiology 216 (3) (2000) 698–703.
[7] D. Hanahan, R.A. Weinberg, Hallmarks of cancer: the next generation, Cell 144 (5) (2011) 646–674.
[8] A. Sreekumar, L.M. Poisson, T.M. Rajendiran, A.P. Khan, Q. Cao, J. Yu, B. Laxman, R. Mehra, R.J. Lonigro, Y. Li, M.K. Nyati, A. Ahsan, S. Kalyana-Sundaram, B. Han, X. Cao, J. Byun, G.S. Omenn, D. Ghosh, S. Pennathur, D.C. Alexander, A. Berger, J.R. Shuster, J.T. Wei, S. Varambally, C. Beecher, A.M. Chinnaiyan, Metabolomic profiles delineate potential role for sarcosine in prostate cancer progression, Nature 457 (7231) (2009) 910–914.
[9] R.J. DeBerardinis, J.J. Lum, G. Hatzivassiliou, C.B. Thompson, The biology of cancer: metabolic reprogramming fuels cell growth and proliferation, Cell Metab. 7 (1) (2008) 11–20.
[10] N.K. Talari, M. Panigrahi, S. Madigubba, S. Challa, P.B. Phanithi, Altered tryptophan metabolism in human meningioma, J. Neurooncol. (2016).
[11] M. Jain, R. Nilsson, S. Sharma, N. Madhusudhan, T. Kitami, A.L. Souza, R. Kafri, M.W. Kirschner, C.B. Clish, V.K. Mootha, Metabolite profiling identifies a key role for glycine in rapid cancer cell proliferation, Science 336 (6084) (2012) 1040–1044.
[12] W.C. Zhang, N. Shyh-Chang, H. Yang, A. Rai, S. Umashankar, S. Ma, B.S. Soh, L.L. Sun, B.C. Tai, M.E. Nga, K.K. Bhakoo, S.R. Jayapal, M. Nichane, Q. Yu, D.A. Ahmed, C. Tan, W.P. Sing, J. Tam, A. Thirugananam, M.S. Noghabi, Y.H. Pang, H.S. Ang, W. Mitchell, P. Robson, P. Kaldis, R.A. Soo, S. Swarup, E.H. Lim, B. Lim, Glycine decarboxylase activity drives non-small cell lung cancer tumor-initiating cells and tumorigenesis, Cell 148 (1–2) (2012) 259–272.
[13] D. Kim, B.P. Fiske, K. Birsoy, E. Freinkman, K. Kami, R.L. Possemato, Y. Chudnovsky, M.E. Pacold, W.W. Chen, J.R. Cantor, L.M. Shelton, D.Y. Gui, M. Kwon, S.H. Ramkissoon, K.L. Ligon, S.W. Kang, M. Snuderl, M.G. Vander Heiden, D.M. Sabatini, SHMT2 drives glioma cell survival in ischaemia but imposes a dependence on glycine clearance, Nature 520 (7547) (2015) 363–367.
[14] H.L. Min, J. Kim, W.H. Kim, B.G. Jang, M.A. Kim, Epigenetic silencing of the putative tumor suppressor gene GLDC (glycine dehydrogenase) in gastric carcinoma, Anticancer Res. 36 (1) (2016) 179–187.
[15] M.A. Swanson, C.R. Coughlin Jr., G.H. Scharer, H.J. Szerlong, K.J. Bjoraker, E.B. Spector, G. Creadon-Swindell, V. Mahieu, G. Matthijs, J.B. Hennermann, D.A. Applegarth, J.R. Toone, S. Tong, K. Williams, J.L. Van Hove, Biochemical and molecular predictors for prognosis in nonketotic hyperglycinemia, Ann. Neurol. 78 (4) (2015) 606–618.
[16] A.S. Tibbetts, D.R. Appling, Compartmentalization of Mammalian folate-mediated one-carbon metabolism, Annu. Rev. Nutr. 30 (2010) 57–81.
[17] Y.J. Pai, K.Y. Leung, D. Savery, T. Hutchin, H. Prunty, S. Heales, M.E. Brosnan, J.T. Brosnan, A.J. Copp, N.D. Greene, Glycine decarboxylase deficiency causes neural tube defects and features of non-ketotic hyperglycinemia in mice, Nat. Commun. 6 (2015) 6388.
[18] A. Meister, S.S. Tate, Glutathione and related gamma-glutamyl compounds: biosynthesis and utilization, Annu. Rev. Biochem. 45 (1976) 559–604.
[19] G. Cohen, P. Hochstein, Glutathione peroxidase: the primary agent for the elimination of hydrogen peroxide in erythrocytes, Biochemistry 2 (1963) 1420–1428.
[20] H.M. Kim, W.H. Jung, J.S. Koo, Site-specific metabolic phenotypes in metastatic breast cancer, J. Transl. Med. 12 (2014) 354.
[21] W.Y. Sun, H.M. Kim, W.H. Jung, J.S. Koo, Expression of serine/glycine metabolism-related proteins is different according to the thyroid cancer subtype, J. Transl. Med. 14 (1) (2016) 168.
[22] C.C. Woo, W.C. Chen, X.Q. Teo, G.K. Radda, P.T. Lee, Downregulating serine hydroxymethyltransferase 2 (SHMT2) suppresses tumorigenesis in human hepatocellular carcinoma, Oncotarget 7 (33) (2016) 53005–53017.
[23] Y. Li, Z.Y. Tang, S.L. Ye, Y.K. Liu, J. Chen, Q. Xue, J. Chen, D.M. Gao, W.H. Bao, Establishment of cell clones with different metastatic potential from the metastatic hepatocellular carcinoma cell line MHCC97, World J. Gastroenterol. 7 (5) (2001) 630–636.
[24] F.X. Sun, Z.Y. Tang, K.D. Lui, S.L. Ye, Q. Xue, D.M. Gao, Z.C. Ma, Establishment of a metastatic model of human hepatocellular carcinoma in nude mice via orthotopic implantation of histologically intact tissues, Int. J. Cancer 66 (2) (1996) 239–243.
[25] L. Xia, W. Huang, D. Tian, Z. Chen, L. Zhang, Y. Li, H. Hu, J. Liu, Z. Chen, G. Tang, J. Dou, S. Sha, B. Xu, C. Liu, J. Ma, S. Zhang, M. Li, D. Fan, Y. Nie, K. Wu, ACP5, a direct transcriptional target of FoxM1, promotes tumor metastasis and indicates poor prognosis in hepatocellular carcinoma, Oncogene 33 (11) (2014) 1395–1406.
[26] H. Zhuang, M.Y. Zhao, K.W. Hei, B.C. Yang, L. Sun, X. Du, Y.M. Li, Aberrant expression of pim-3 promotes proliferation and migration of ovarian cancer cells, Asian Pac. J. Cancer Prev. 16 (8) (2015) 3325–3331.
[27] R. Sun, P. Gao, L. Chen, D. Ma, J. Wang, J.J. Oppenheim, N. Zhang, Protein kinase C zeta is required for epidermal growth factor-induced chemotaxis of human breast cancer cells, Cancer Res. 65 (4) (2005) 1433–1441.
[28] J. Yao, L. Liang, S. Huang, J. Ding, N. Tan, Y. Zhao, M. Yan, C. Ge, Z. Zhang, T. Chen, D. Wan, M. Yao, J. Li, J. Gu, X. He, MicroRNA-30d promotes tumor invasion and metastasis by targeting Galphai2 in hepatocellular carcinoma, Hepatology 51 (3) (2010) 846–856.
[29] J. Gao, B.A. Aksoy, U. Dogrusoz, G. Dresdner, B. Gross, S.O. Sumer, Y. Sun, A. Jacobsen, R. Sinha, E. Larsson, E. Cerami, C. Sander, N. Schultz, Integrative analysis of complex cancer genomics and clinical profiles using the cBioPortal, Sci. Signal. 6 (269) (2013) pl1.
[30] B. Yang, Y. Liu, J. Zhao, K. Hei, H. Zhuang, Q. Li, W. Wei, R. Chen, N. Zhang, Y. Li, Ectopic overexpression of filamin C scaffolds MEK1/2 and ERK1/2 to promote the progression of human hepatocellular carcinoma, Cancer Lett. 388 (2017) 167–176.
[31] H.R. Dawe, L.S. Minamide, J.R. Bamburg, L.P. Cramer, ADF/cofilin controls cell polarity during fibroblast migration, Curr. Biol. 13 (3) (2003) 252–257.
[32] W. Wang, R. Eddy, J. Condeelis, The cofilin pathway in breast cancer invasion and metastasis, Nat. Rev. Cancer 7 (6) (2007) 429–440.
[33] N. Yang, O. Higuchi, K. Ohashi, K. Nagata, A. Wada, K. Kangawa, E. Nishida, K. Mizuno, Cofilin phosphorylation by LIM-kinase 1 and its role in Rac-mediated actin reorganization, Nature 393 (6687) (1998) 809–812.
[34] B.V. McConnell, K. Koto, A. Gutierrez-Hartmann, Nuclear and cytoplasmic LIMK1 enhances human breast cancer progression, Mol. Cancer 10 (2011) 75.
[35] Y. Yoo, H.J. Ho, C. Wang, J.L. Guan, Tyrosine phosphorylation of cofilin at Y68 by v-Src leads to its degradation through ubiquitin-proteasome pathway, Oncogene 29 (2) (2010) 263–272.
[36] J.T. Skamarauskas, F. Oakley, F.E. Smith, C. Bawn, M. Dunn, D.S. Vidler, M. Clemence, P.G. Blain, R. Taylor, M.P. Gamcsik, P.E. Thelwall, Noninvasive in vivo magnetic resonance measures of glutathione synthesis in human and rat liver as an oxidative stress biomarker, Hepatology 59 (6) (2014) 2321–2330.
[37] J. Jahngen-Hodge, M.S. Obin, X. Gong, F. Shang, T.R. Nowell Jr., J. Gong, H. Abasi, J. Blumberg, A. Taylor, Regulation of ubiquitin-conjugating enzymes by glutathione following oxidative stress, J. Biol. Chem. 272 (45) (1997) 28218–28226.
[38] M. Obin, F. Shang, X. Gong, G. Handelman, J. Blumberg, A. Taylor, Redox regulation of ubiquitin-conjugating enzymes: mechanistic insights using the thiol-specific oxidant diamide, FASEB J. 12 (7) (1998) 561–569.

[39] P. Korge, G. Calmettes, J.N. Weiss, Increased reactive oxygen species production during reductive stress: the roles of mitochondrial glutathione and thioredoxin reductases, Biochim. Biophys. Acta 1847 (6–7) (2015) 514–525.
[40] J. Zhang, K.S. Ahn, C. Kim, M.K. Shanmugam, K.S. Siveen, F. Arfuso, R.P. Samym, A. Deivasigamanim, L.H. Lim, L. Wang, B.C. Goh, A.P. Kumar, K.M. Hui, G. Sethi, Nimbolide-induced oxidative stress abrogates STAT3 signaling cascade and inhibits tumor growth in transgenic adenocarcinoma of mouse prostate model, Antioxid. Redox Signal. 24 (11) (2016) 575–589.
[41] P. Chelikani, I. Fita, P.C. Loewen, Diversity of structures and properties among catalases, Cell Mol. Life Sci. 61 (2) (2004) 192–208.
[42] M. Peiris-Pages, U.E. Martinez-Outschoorn, F. Sotgia, M.P. Lisanti, Metastasis and oxidative stress: are antioxidants a metabolic driver of progression? Cell Metab. 22 (6) (2015) 956–958.
[43] N. Taulet, V.D. Delorme-Walker, C. DerMardirossian, Reactive oxygen species regulate protrusion efficiency by controlling actin dynamics, PLoS One 7 (8) (2012) e41342.
[44] Y.M. Go, M. Orr, D.P. Jones, Actin cytoskeleton redox proteome oxidation by cadmium, Am. J. Physiol. Lung Cell Mol. Physiol. 305 (11) (2013) L831–L843.
[45] M.F. Montenegro, A. Valdivia, A. Smolensky, K. Verma, W.R. Taylor, A. San Martin, Nox4-dependent activation of cofilin mediates VSMC reorientation in response to cyclic stretching, Free Radic. Biol. Med. 85 (2015) 288–294.
[46] F. Klamt, S. Zdanov, R.L. Levine, A. Pariser, Y. Zhang, B. Zhang, L.R. Yu, T.D. Veenstra, E. Shacter, Oxidant-induced apoptosis is mediated by oxidation of the actin-regulatory protein cofilin, Nat. Cell Biol. 11 (10) (2009) 1241–1246.
[47] J.M. Cameron, M. Gabrielsen, Y.H. Chim, J. Munro, E.J. McGhee, D. Sumpton, P. Eaton, K.I. Anderson, H. Yin, M.F. Olson, Polarized cell motility induces hydrogen peroxide to inhibit cofilin via cysteine oxidation, Curr. Biol. 25 (11) (2015) 1520–1525.
[48] J.S. Kim, T.Y. Huang, G.M. Bokoch, Reactive oxygen species regulate a slingshot-cofilin activation pathway, Mol. Biol. Cell 20 (11) (2009) 2650–2660.
[49] E.E. Grintsevich, H.G. Yesilyurt, S.K. Rich, R.J. Hung, J.R. Terman, E. Reisler, F-actin dismantling through a redox-driven synergy between Mical and cofilin, Nat. Cell Biol. 18 (8) (2016) 876–885.
[50] H.J. Kim, S. Ha, H.Y. Lee, K.J. Lee, ROSics: chemistry and proteomics of cysteine modifications in redox biology, Mass Spectrom. Rev. 34 (2) (2015) 184–208.
[51] M. Fratelli, H. Demol, M. Puype, S. Casagrande, I. Eberini, M. Salmona, V. Bonetto, M. Mengozzi, F. Duffieux, E. Miclet, A. Bachi, J. Vandekerckhove, E. Gianazza, P. Ghezzi, Identification by redox proteomics of glutathionylated proteins in oxidatively stressed human T lymphocytes, Proc. Natl. Acad. Sci. USA 99 (6) (2002) 3505–3510.
[52] M.M. Stacey, S.L. Cuddihy, M.B. Hampton, C.C. Winterbourn, Protein thiol oxidation and formation of S-glutathionylated cyclophilin A in cells exposed to chloramines and hypochlorous acid, Arch. Biochem. Biophys. 527 (1) (2012) 45–54.
[53] H.S. Kim, S.L. Ullevig, H.N. Nguyen, D. Vanegas, R. Asmis, Redox regulation of 14-3-3zeta controls monocyte migration, Arterioscler. Thromb. Vasc. Biol. 34 (7) (2014) 1514–1521.
[54] I.A. Voutsadakis, The ubiquitin-proteasome system and signal transduction pathways regulating Epithelial Mesenchymal transition of cancer, J. Biomed. Sci. 19 (2012) 67.
[55] G.L. Semenza, Hypoxia-inducible factors: coupling glucose metabolism and redox regulation with induction of the breast cancer stem cell phenotype, EMBO J. 36 (3) (2017) 252–259.